IMPROVEMENT OF THE CONVECTION HEAT TRANSFER FOR THE PRODUCTION OF COKE ANODE OF AN ALUMINUM INDUSTRY

Martins, M. F.
Universidade Federal do Pará, Departamento de Engenharia Mecânica. Campus Universitário do Guamá – Av. Augusto Corrêa, 01 – 67.750-930 – Belém-PA. marciofm@ufpa.br

Rendeiro, G.
Universidade Federal do Pará, Departamento de Engenharia Mecânica. Campus Universitário do Guamá – Av. Augusto Corrêa, 01 – 67.750-930 – Belém-PA.

Dias, L. De O.
Universidade Federal do Pará, Departamento de Engenharia Mecânica. Campus Universitário do Guamá – Av. Augusto Corrêa, 01 – 67.750-930 – Belém-PA. Leonardodias22@zipmail.com.br

Da Cunha, F. A.
Universidade Federal do Pará, Departamento de Engenharia Mecânica. Campus Universitário do Guamá – Av. Augusto Corrêa, 01 – 67.750-930 – Belém-PA. alfaia@ufpa.br

Abstract. *Cooking is the most expensive step of the process of making the anode used for the aluminum production. The cooking improves the anode mechanical strength, electrical conductivity, resistance to oxidation and CO_2 reactivity. Thermal conductivity is one of the most important properties of the anode, and it increases exponentially with the cooking temperature. This work studied how to improve the quality of the anode used in aluminum industry by searching for the best temperature profiles of the cooking pit during anode production. In order to achieve the best temperature configuration, numerical simulations were performed and also a scale model of the anode cooking pit was built reproducing real conditions. Improvements of the anode properties were accounted for by introducing chicanes inside the combustion chamber achieving better convection heat transfer coefficient. Simple boundary conditions were used such as convection and radiation heat transfer at two faces and temperature specified at the other three faces of the anode. The radiation between the anode and the wall was neglected when compared to the order of magnitude of convection and conduction. Numerical solution for the heat transfer equations was obtained by Classical Integral Transform. In order to obtain the experimental temperature profile and increase the convection heat transfer coefficient of the heating chambers, a scale model of the cooking pit was built. Temperature was measured inside the heating chamber and the convection heat transfer coefficient was then inferred.*

Keywords *Coke Anode Heat Transfer, Anode cooking, Integral Transform, Anode Experimental Analysis.*

1. Introduction

Coke anodes are crucial for the aluminum fabrication process, Kocaef *et al* (1996). Therefore, aluminum industries are also anode-cooking plants. Due to its importance the anode properties have a great influence on the efficiency of aluminum production.

The coke anode is basically a polycrystalline carbon body made of coke and pitch and is cooked in open ovens. The reasons for the cooking process are:

- To improve the mechanical strength to receive pin supports and resist to *thermal changes.*
- To increase the electrical conductivity decreasing the voltage inside the electrolytic chamber.
- To improve the resistance to CO2 reaction (during electrolysis) and resistance to oxidation (in contact with air).

The increase of calcinations temperatures improves the anode properties up to a limit value and consequently improves its efficiency during aluminum production. Reactivity to CO2, density and electrical resistance are some of the properties influencing the anode efficiency.

Thermal conductivity is one of the most important properties of the anode, and it increases exponentially with the cooking temperature. However, an excessive increase of cooking temperature makes the anode more susceptible to oxidation.

Considering the importance of the anode and knowing that improving the anode properties will result in a great energy reduction for the aluminum production, it is important to study the best way of cooking the anodes, simulating and proposing the best study about heat exchange coefficient and temperature profile for open ovens.

The oven used for the anode cooking of several aluminum industries has 7 combustion chambers and 6 pits. The oven has the capacity to cook 12 anodes. A simplified mathematical model simulated only two combustion chambers and one cooking pit since the configuration of the oven is totally symmetric Fig. (1).

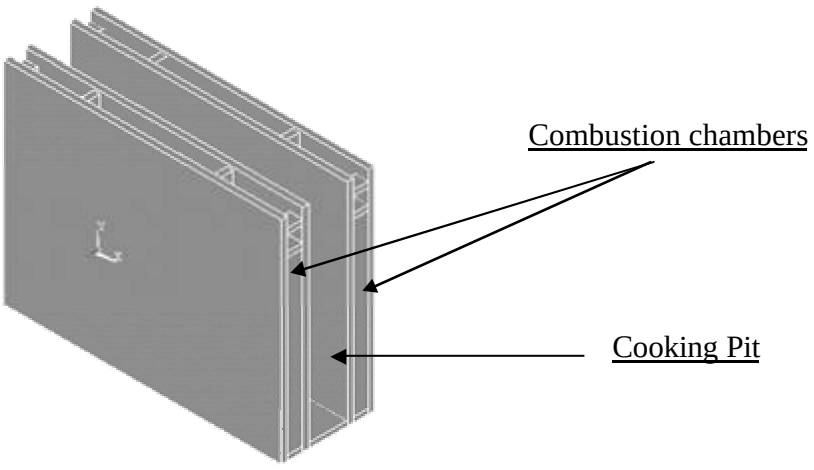

Figura1 – Schematic front view and 3D view of the combustion chamber and cooking pit.

The geometry of the combustion chambers and cooking pit is very simple; Fig. (2) shows the schematic of the combustion chambers and pit used to numerically simulate the heat transfer. Cartesian coordinates and parallelepiped geometry were considered for the numerical simulation. Boundary conditions for the model are shown in Fig. (3), where convection and radiation heat transfer occur at two faces and temperature is specified at the other three faces of the anode. Steady state conditions are

assumed, internal energy source or well are disregarded, thermal conductivity is considered constant and the radiation between the anode and the wall is ignored because its order of magnitude compared to convection and conduction.

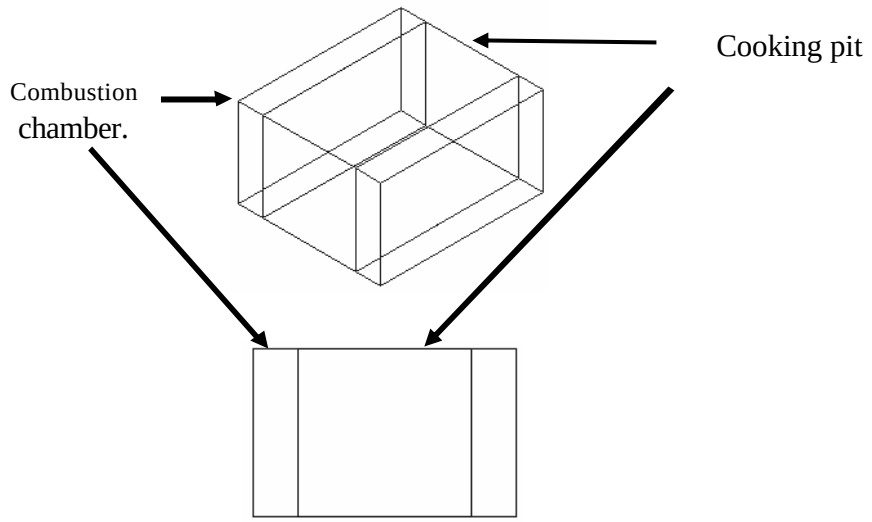

Fig. (2) – Schematic front view and 3D view of the combustion chamber and cooking pit.

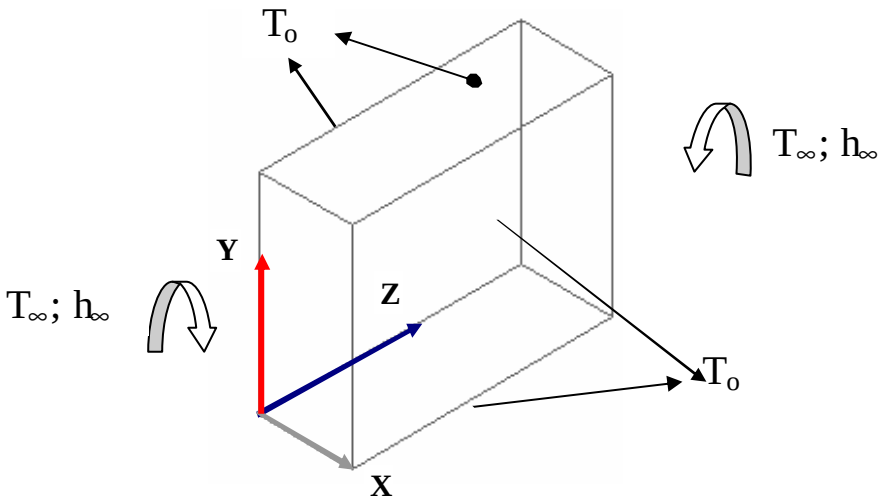

Fig. (3) – Boundary conditions for the numerical problem.

Considering the simplifications and boundary conditions, the anode cooking heat transfer is modeled by Eq. (1):

$$\frac{\partial^2 T}{\partial x^2}+\frac{\partial^2 T}{\partial y^2}+\frac{\partial^2 T}{\partial z^2}=0 \ , \ 0 < x < a, \quad 0 < y < b, \quad 0 < z < c \tag{1}$$

$$T(x=0,y,z)=T(x=a,y,z)=T_o \tag{2}$$

$$T(x, y = 0, z) = T(x, y = b, z) = T_o \tag{3}$$

$$-k\frac{\partial T}{\partial z} + h_\infty (T - T_\infty) = 0 \quad \text{em } z = 0 \tag{4}$$

$$k\frac{\partial T}{\partial z} + h_\infty (T - T_\infty) = 0 \quad \text{em } z = c \tag{5}$$

The dimensionless groups are defined as:

$$? = T - T_o \;\; ; \;\; \theta_\infty = T_o - T_\infty \;\; , \;\; B_i = \frac{h_\infty}{k} \;\; , \;\; \gamma = B_i \theta_\infty \tag{6}$$

So Eq. (1) to Eq. (5) can be written in a dimensionless form:

$$\frac{\partial^2 \theta}{\partial x^2} + \frac{\partial^2 \theta}{\partial y^2} + \frac{\partial^2 \theta}{\partial z^2} = 0, \quad 0 < x < a \quad 0 < y < b \quad 0 < z < c \tag{7}$$

$$q(x = 0, y, z) = q(x = a, y, z) = 0 \tag{8}$$

$$q(x, y = 0, z) = q(x, y = b, z) = 0 \tag{9}$$

$$-\frac{\partial q}{\partial z} + B_i q = -g \quad \text{em} \quad z = 0 \tag{10}$$

$$\frac{\partial q}{\partial Z} + B_i q = -g \quad \text{em} \quad z = c \tag{11}$$

2. Classical Integral Transform Technique (CITT) applied to the problem

Classical Integral Transform method (CITT) was used for the solution of the equations, Cotta (1998). Temperatures for the three planes (xy,xz,yz) were calculated using the following CITT steps:

2.1. Auxiliary problems

Applying the separation of variables to the homogeneous problem of Eq. (7) to Eq. (11) can be rewritten as auxiliary equations in x and y directions:

$\begin{cases} \frac{d^2\Psi(x)}{dx^2} + \mu_i^2 \Psi(x) = 0 \\ \Psi(0) = 0, \quad \Psi(a) = 0 \end{cases}$ (12)	$\begin{cases} \frac{d^2\Phi(y)}{dy} + \lambda_m^2 \Phi(y) = 0 \\ \Phi(0) = 0, \quad \Phi(b) = 0 \end{cases}$ (14)
onde,	onde,

$\Psi(x) = \mathrm{Sin}(\mu_i x)$ $\mu_i = \frac{i\pi}{a};\ N_i = \frac{a}{2}$ (13) $\tilde{\Psi}_i(x) = \frac{\mathrm{Sin}(\mu_i x)}{\sqrt{N_i}}$	$\Phi(y) = \mathrm{Sin}(\lambda_m y)$ $\lambda_m = \frac{m\pi}{b};\ M_m = \frac{b}{2}$ (15) $\tilde{\Phi}_m(y) = \frac{\mathrm{Sin}(\lambda_m y)}{\sqrt{M_m}}$

2.2. Development of the Integral Transform Pairs

The solution can be obtained from the desired potencial ? in terms of the eigenfunctions $\tilde{\Psi}_i(x)$ e $\tilde{\Phi}_m(y)$ of the auxiliary problem.

$$\theta(x,y,z) = \sum_{i=1}^{\infty}\sum_{m=1}^{\infty} \tilde{\Psi}_i(x)\tilde{\Phi}_m(y)F(z) \tag{16}$$

Since eigenfunctions $\tilde{\Psi}_i(x)$ e $\tilde{\Phi}_m(y)$ are orthogonal the following integral transform pairs can be defined:

$$\bar{\bar{\theta}}_{im}(z) = \int_0^a\int_0^b \tilde{\Psi}_i(x)\tilde{\Phi}_m(y)\theta(x,y,z)dxdy \quad \text{Integral Transform} \tag{17}$$

$$\theta(x,y,z) = \sum_{i=1}^{\infty}\sum_{m=1}^{\infty} \tilde{\Psi}_i(x)\tilde{\Phi}_m(y)\bar{\bar{\theta}}_{im}(z) \quad \text{Inversion Formula} \tag{18}$$

2.3. Integral Transform of the Partial Differential Equation

Equation (7) was multiplied by eigen functions $\tilde{\Psi}_i(x)$ e $\tilde{\Phi}_m(y)$ and resulting equation was integrated over the domain.

$$\int_0^a\int_0^b \tilde{\Psi}_i(x)\tilde{\Phi}_m(x)\left\{\frac{\partial^2\theta}{\partial x^2} + \frac{\partial^2\theta}{\partial y^2} + \frac{\partial^2\theta}{\partial z^2} = 0\right\}dxdy \tag{19}$$

So the partial differential equation Eq. (1) and its boundary conditions Eq. (2) to Eq. (5) were transformed into uncoupled ordinary equations.

$$\begin{cases} \dfrac{d^2\bar{\bar{\theta}}_{im}(Z)}{dz^2} - \Delta_{im}^2 \bar{\bar{\theta}}_{im}(z) = 0; \quad 0 < z < c \\ -\dfrac{d\bar{\bar{\theta}}_{im}(z)}{dz} + B_i \bar{\bar{\theta}}_{im}(z) = -\gamma \tilde{f}_i \tilde{g}_m; \quad z = 0 \\ \dfrac{d\bar{\bar{\theta}}_{im}(z)}{dz} + B_i \bar{\bar{\theta}}_{im}(z) = -\gamma \tilde{f}_i \tilde{g}_m; \quad z = c \end{cases} \tag{20}$$

where

$$\tilde{f}_i = \int_0^a \tilde{\Psi}_i(x)dx = \int_0^a \frac{Sin(\mu_i x)}{\sqrt{N_i}} dx = \frac{1 - Cos(\mu_i a)}{\mu_i \sqrt{N_i}} = \frac{1-(-1)^i}{\mu_i \sqrt{N_i}} \tag{21}$$

$$\tilde{g}_m = \int_0^b \tilde{\Phi}_m(y)dy = \int_0^b \frac{Sin(\lambda_m y)}{\sqrt{M_m}} dY = \frac{1 - Cos(\lambda_m b)}{\lambda_m \sqrt{M_m}} = \frac{1-(-1)^m}{\lambda_m \sqrt{M_m}} \tag{22}$$

$$\Delta_{im} = \sqrt{\mu_i^2 + \lambda_m^2} \tag{23}$$

2.4. Solution of the Ordinary Differential Equation System

For the solution of the system of Eq. (20) to Eq. (23) it is proposed:

$$\bar{\bar{\theta}}_{im}(z) = \exp(Pz) \tag{24}$$

Replacing Eq. (24) into Eq. (20) the solution of the differential ordinary equation can be obtained by:

$$P = \pm \Delta_{im} \tag{25}$$

With calculated P, the solution for the system is in the form:

$$\bar{\bar{\theta}}_{im}(Z) = C_1 \exp(-\Delta_{im} Z) + C_2 \exp(\Delta_{im} Z) \tag{26}$$

Applying Eq. (26) into boundary conditions Eq. (20) C_1 and C_2can be obtained:

$$C_1 = \frac{\varpi_{im} \exp(\Delta_{im} c)}{B_m [1 + \exp(\Delta_{im} c)] + \Delta_{im} [\exp(\Delta_{im} c) - 1]} \tag{27}$$

$$C_1 = \frac{\varpi_{im}}{B_m\left[1+\exp\left(\Delta_{im}c\right)\right]+\Delta_{im}\left[\exp\left(\Delta_{im}c\right)-1\right]} \tag{28}$$

$$\varpi_{im} = -\gamma\tilde{f}_i\tilde{g}_m \tag{29}$$

2.5. Recall of the inversion formulae to provide the temperature values

The following inversion formulae is used to provide the complete temperature field:

$$\theta(x,y,z) = \sum_{i=1}^{\infty}\sum_{m=1}^{\infty}\tilde{\Psi}_i(x)\tilde{\Phi}_m(y)\bar{\bar{\theta}}_{im}(z) \tag{30}$$

3. Experimental analysis

An experimental study was developed to compare the numerical model estimates with experimental results. The experimental apparatus was comprised of a scale model of the real combustion chamber and anode cooking pit Type J thermocouples were used to measure 13 temperature points in the anode Fig. (4). The measured temperatures were used to evaluate the heat transfer from the combustion chamber to the anode. Temperatures of the combustion chamber were also taken using 12 type J thermocouples Fig. (5).

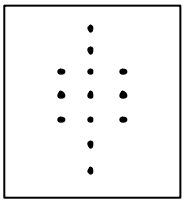

Fig. (4) – Sites for the anode temperature measurements.

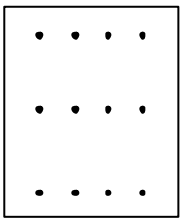

Fig. (5) – Sites for the combustion chamber temperature measurements.

Propane was burned to elevate the temperature in the combustion chamber Fig. (6) and chicanes were used to improve the convection heat transfer from the combustion chamber to anode cooking pit.

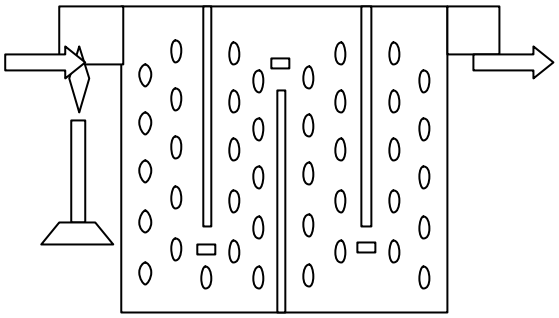

Fig. (6) – Combustion chamber heating and chicanes.

4. Results and conclusions

For the Anode, numerical and experimental temperature results agree within 10% for the (x, y) plane. Figure (7) shows the numerical (line) and experimental (symbols) results for the center line of the (x, y) plane. Temperatures were also calculated for the (x, z) and (y, z) planes but the comparisons with experimental measurements could not be performed as the small dimensions of the scale model resulted in a lack of resolution for the thermocouple positioning. Figure (8), Fig. (9) and Fig. (10) show numerical results using color pattern.

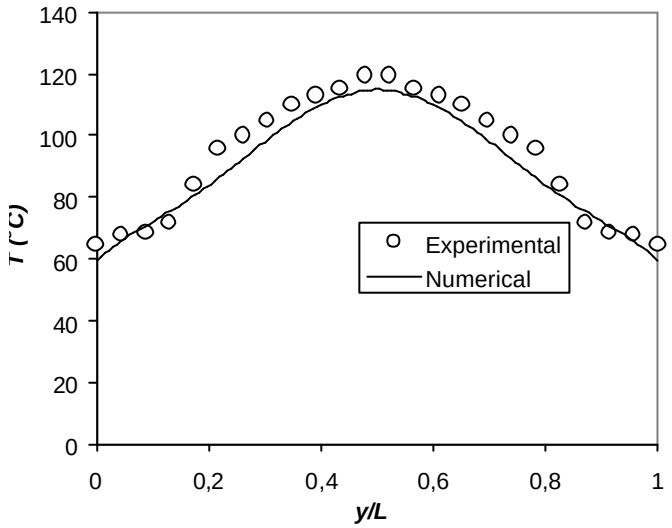

Fig. (7) – Temperature profile for the center line of the (x, y) plane, with z = c/2.

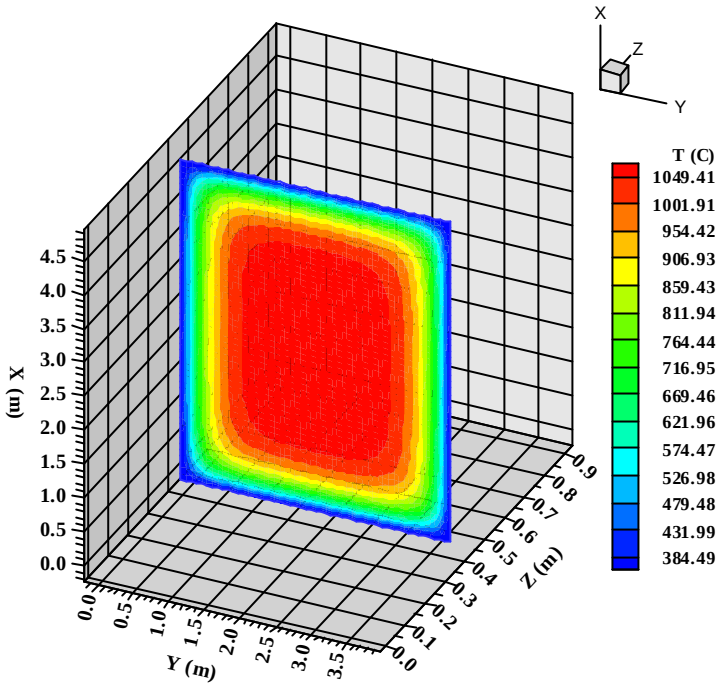

Fig. (7) – Colored temperature profile for the (x, y) plane, with z = c/2.

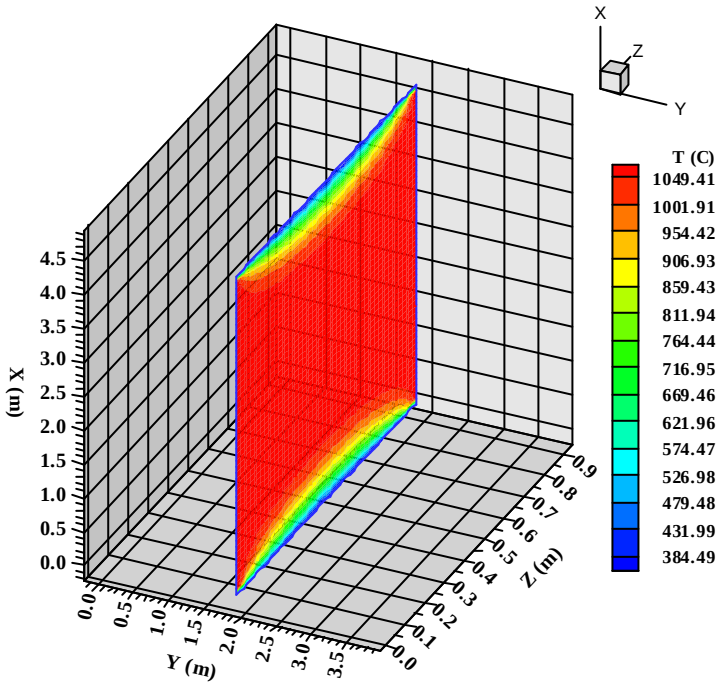

Fig. (8) – Colored temperature profile for the (x, z) plane, with y = b/2.

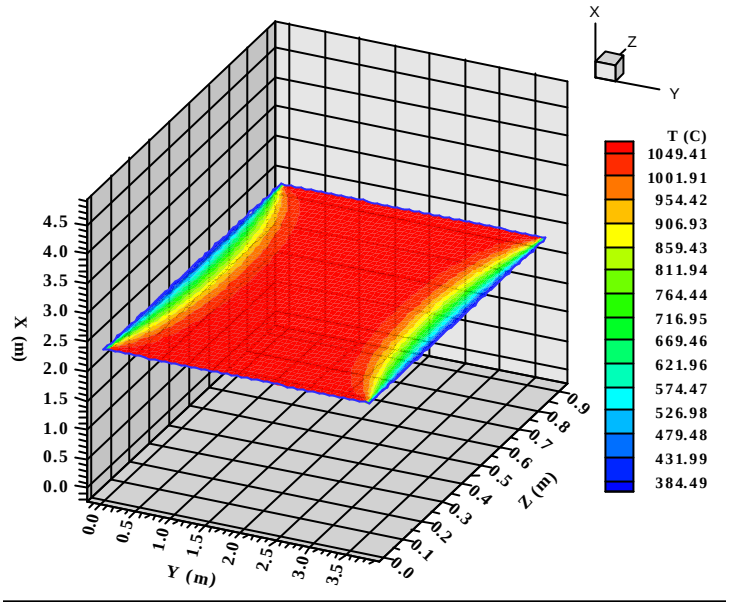

Fig. (9) – Colored temperature profile for the (y, z) plane, with x = a/2.

In accordance with the used mathematical analysis and with the gotten experimental results, the methodology used experimental technique and revealed consistent. However, to improve and to uniformizar the profile of temperature in the oven we indicate a study CFD, to simulate the draining of the fluid in the interior of the chamber, and consequently it will bring improvements of the global coefficient of transference involved in the process - Thomas *et al*(1999). High values of speed imply in the formation of recirculation in some points of the combustion chamber - Thomas *et al* (1999). Therefore, one becomes necessary to advance in the research being used considered computational models already in literature.

5. References

Cotta, R. M. and Mikhailov, M. D., 1997, "Heat Conduction – Lumped Analysis, Integral Transforms, Symbolic Computation". John Wiley & Sons, New York, USA.

Cotta, R. M., 1998, "The Integral Transform Method in Thermal and Fluids Science and Engineering". Begell House, New York, USA.

Fisher, W.K., Keller, F., Perruchoud, R.C. and Oderboltz, S., Baking Parameters and Resultinganode Quality. Aime Ligth Metals, 1993, PP 739-745 (1993).

J.Bos - G. Bouzat – J. Colin de Verdière – B. Fève – J.C.Rotger. Numerical Simulation, Tools to Design and Optimize Smelting Technology.Ligth Metals, 1998.

J.C Thomas, P.Breme, J.C Rotger, F. Cha rmier, J.G Ameeri. Conversion of a Closed Furnace to The Open Type Technology at Aluminium BAHRAIN. Light Metals. 1999.

Meier, M. W.; Cracking Behaviour of Anodes, edition a la carte sa, Switzerland, 1996.

Victor L. Streeter, E. Benjamin Wylie, Mecanica dos Fluidos, 7ª Edição, Brasil, McGraw-Hill do Brasil, Ltda. 1982. 166.

Y.S. Kocaefe, E. Dernedde, D. Kocaefe, R. Ouellet, Q. Jiao, W.F. Crowell. A 3d Methematical Model For The Horizontal Anode Banking Furnace. Ligth Metals, 1996.